Photoproduct Characterization and Dynamics in the 248 nm Photolysis of CH_3I Thin Films on Ag(111)

S. R. Coon,† K. B. Myli, and V. H. Grassian*

Department of Chemistry, University of Iowa, Iowa City, Iowa 52242

Received: June 28, 1995; In Final Form: August 28, 1995®

The 248 nm photochemistry of methyl iodide thin films was studied using reflection absorption infrared spectroscopy (RAIRS), temperature programmed desorption (TPD), and time-of-flight quadrupole mass spectrometry (TOF-QMS). The formation of predominantly CH_2I_2 and CH_4 and some C_2H_6, CH_3CH_2I, CHI_3, and I_2 photoproducts retained in the film was characterized by RAIRS and TPD. The integrated areas of the IR absorption bands for the two major photoproducts, CH_2I_2 and CH_4, increase to a maximum and then decrease as photolysis of the film proceeds. A cross section for the loss of CH_3I by 248 nm photolysis of the film was measured to be $(1.6 \pm 0.1) \times 10^{-19}$ cm^2, approximately 1 order of magnitude lower than the gas-phase cross section. At all laser fluences used in this study, CH_3, I, and CH_3I were ejected into the gas phase. The CH_3 TOF distribution showed the signature of gas-phase CH_3I photodissociation dynamics—two sharp peaks corresponding to the production of iodine atoms in the $I(^2P_{3/2})$ and $I^*(^2P_{1/2})$ states. The TOF distributions of I and CH_3I were fit by Maxwell-Boltzmann distributions corresponding to temperatures of 1400 and 1170 K, respectively. Three other species—CH_4, I_2 and CH_2I_2—were observed in TOF-QMS, but only at higher laser fluences. It was determined that the I_2 and CH_2I_2 species are most likely fragments of a larger molecule, perhaps a cluster species, that photodesorbs as the film becomes enriched with photoproducts. The mechanism for CH_4 photoejection appears to be of a different nature. The photochemistry of methyl iodide thin films can be understood in terms of a combination of photoprocesses occurring in the film and at the film surface.

Introduction

The photodissociation of methyl iodide has received much experimental attention. In the gas phase, photodissociation of CH_3I at 248 nm produces methyl radicals and iodine atoms in both the $I(^2P_{3/2})$ and $I^*(^2P_{1/2})$ states through an $n \rightarrow \sigma^*$ transition. These direct photoproducts can react with each other and with other methyl iodide molecules to form various molecular species. Harris and Willard[1] reported the formation of CH_4, CH_2I_2, CHI_3, C_2H_6, C_2H_4, and I_2 after photolysis of gas-phase CH_3I with a quartz mercury arc lamp. Souffie et al.[2] established that both methane and ethane were formed by reactions of hot methyl radicals in the 254 nm photolysis of gaseous methyl iodide. Barker, Purnell, and Young studied the photolysis of films of CH_3I at 77 K[3] and saw the formation of many more products, in particular C_2 and C_3 hydrocarbons. They observed that all the photoproducts were primary (i.e., photoproduct formation was directly correlated with loss of CH_3I). Interestingly, they did not observe the formation of CH_2I_2, a major photoproduct in the Harris and Willard gas-phase study. Photolysis of clusters has been used to approach the condensed phase from the level of individual molecules, as well as to investigate ion-molecule reactions.[4-10] The formation of I_2^+ from CH_3I clusters was first observed in multiphoton ionization at 248 nm.[5] Subsequent experiments using single-photon excitation established that I_2 is formed primarily by neutral cluster reactions,[6,8,9] although I_2^+ has also been produced by electron ionization of methyl iodide clusters.[10]

More recently, the photodissociation of multilayers or thin films of methyl iodide adsorbed on various substrates has been investigated.[11-20] These studies have focused on the dynamics of the dissociation by measuring time-of-flight (TOF) distributions of species ejected into the gas phase. At high coverages, greater than approximately five layers, the photochemistry of CH_3I can be understood in terms of a direct excitation mechanism.[11,15,17-19] The nature of the substrate becomes increasingly less important at high coverages. At low coverages, below approximately five layers, the role of the substrate is quite large.[11,21] For metal substrates, such as Ag, dissociative electron attachment processes, an important pathway for photofragmentation of molecules adsorbed on metal surfaces,[22,23,24] dominate the photochemistry of the first few layers.[11,21] For some substrates, such as MgO,[13,14] these substrate-mediated processes become less important. However, the geometry of the adsorbate in the first few layers, e.g., iodine atom in adsorbed methyl iodide bonded to or directed away from the surface, can be influenced by the underlying substrate.[13]

Little attention has been paid to the fate of the species in the film. This work focuses on the gas and film photoproduct formation, as well as the dynamics, of the photochemistry of CH_3I thin films on Ag(111) at 248 nm. Methyl iodide was chosen because of its well-known photochemistry in the gas and condensed phases and in clusters, and its well-characterized surface chemistry and photochemistry on Ag(111) at low coverages.[21,25] The current study shows that the photochemistry that takes place in a molecular film and at the film surface is readily amenable for study with a combination of techniques that probe both the film and the gas phase. A recent study using electron beams for irradiation of methanol films also demonstrates the use of conventional surface science techniques as a probe of radiation-induced chemistry in multilayers.[26]

Experimental Section

The experiments were performed in a 30.5 cm diameter ultrahigh vacuum chamber (base pressure 1.5×10^{-10} Torr) equipped with an electron gun/single pass cylindrical mirror analyzer for Auger electron spectroscopy (AES) and a sputter gun for back-fill sputter cleaning with Ar^+, both from Physical

* Author to whom correspondence should be addressed.
† Current address: Department of Chemistry, University of Northern Iowa, Cedar Falls, IA 50614.
® Abstract published in *Advance ACS Abstracts,* October 15, 1995.

0022-3654/95/2099-16416$09.00/0

Electronics. A UTI 100C quadrupole mass spectrometer was used for residual gas analysis (RGA), temperature programmed desorption (TPD), and time-of-flight quadrupole mass spectrometry (TOF-QMS). The mass spectrometer was housed in a double differentially pumped stainless steel cross attached to the main chamber. Two apertures, ~7 mm in diameter, were placed in line-of-sight of the crystal at distances of 7 and 20 cm from the crystal surface. The center of the ionizer of the mass spectrometer was 24 cm from the crystal surface. The ionizer to surface distance was calibrated using the peak energies of the two sharp methyl peaks in the TOF distribution.[15] These peaks also established the flight time of $m/e = 15$ ions through the quadrupole mass spectrometer as 20.1 μs. The flight times in the QMS of other ions were calculated by scaling by the square root of the mass. With this experimental geometry, the viewing area of the surface by the mass spectrometer is approximately the size of the crystal (12.5 mm diameter) and only species desorbing near the surface normal are detected. For TOF-QMS, the pulses from the high gain electron multiplier of the mass spectrometer were amplified and sent to a multichannel scaler (EG&G Ortec), which discriminates the pulses and counts them as a function of arrival time.

Reflectance absorption infrared spectroscopy (RAIRS) data were obtained by focusing the external beam of a Mattson Galaxy 6021 Fourier transform infrared spectrometer onto the Ag crystal at grazing incidence (approximately 84° from the surface normal). The reflected beam was then focused onto a liquid-nitrogen-cooled external narrowband mercury cadmium telluride detector. The infrared beam entered and exited the chamber through BaF_2 windows. Unless otherwise noted, the RAIR spectra were acquired by averaging 1000 scans at an instrument resolution of 2 cm^{-1}.

The second harmonic of a pulsed (7 ns fwhm) Nd:YAG laser (Continuum YG-661), operated at 10 Hz, was used to pump a dye laser (Continuum). The doubled DCM dye ($\lambda = 323.4$ nm) mixed with the 1064 nm fundamental of the Nd:YAG laser produced 248 nm s-polarized light. For all of the infrared and TPD experiments and most of the TOF experiments, a 1 m focal length quartz lens was placed in the optical path to focus the beam and reexpand it to the size of the silver crystal. The laser fluence at the sample using this arrangement was approximately 0.9 mJ/cm^2 per pulse. The only modification made to the optical path during the course of the experiments was the removal of the beam-expanding lens, resulting in an increase in laser fluence to approximately 3.2 mJ/cm^2 per pulse. The laser beam was incident on the sample at an angle of 30° from the surface normal, entering and exiting the chamber through sapphire windows.

The Ag(111) crystal face was polished using standard techniques. The crystal was mounted in a ring-mount-style Ta assembly, with Ta heating leads spot-welded to the rear of the assembly. The heating leads were also in thermal contact with a liquid nitrogen reservoir. The sample could be cooled to 100 K and resistively heated to 900 K. The temperature was measured by a thermocouple pressed into a small hole near the edge of the crystal. Sputter cleaning and annealing to 800 K produced a clean surface as determined by AES.

Methyl iodide (Aldrich, 99.5% purity) and methylene iodide (Aldrich, 99% purity) were stored in the dark at 277 K. Both samples went through several freeze, pump, thaw cycles before being admitted to the chamber. No impurities were detected by mass spectrometry. The crystal was dosed by back-filling the chamber while the sample was held at 100 K. For methyl iodide, one monolayer (1 ML) exposure was determined from TPD to be 3 langmuirs (1 langmuir = 1×10^{-6} Torrs).

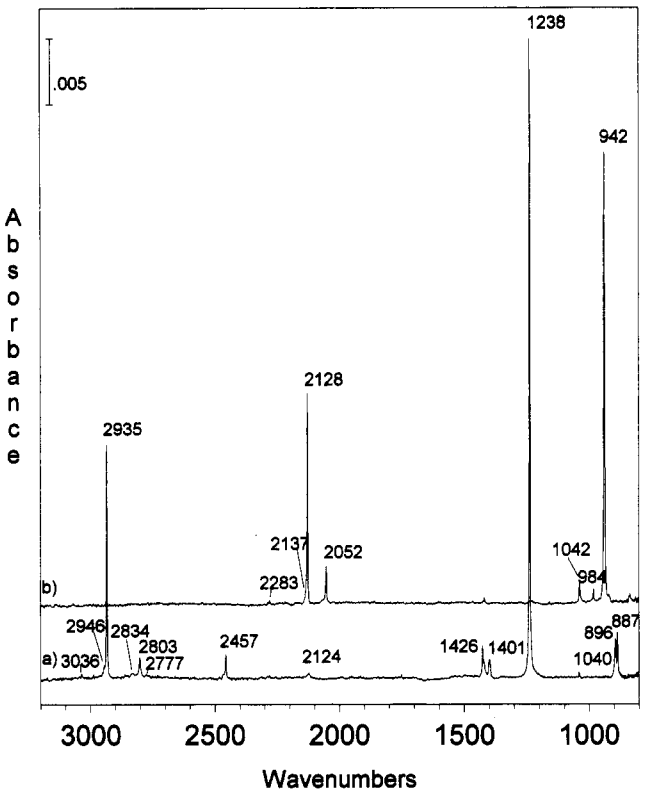

Figure 1. 2 cm^{-1} resolution RAIR spectra of (a) CH_3I and (b) CD_3I thin films adsorbed on Ag(111).

Results

Approximately 70 ML of CH_3I was adsorbed onto a Ag(111) surface and then photolyzed with 248 nm photons. Species remaining in the film and on the Ag surface after photolysis were monitored with RAIRS and TPD. Species ejected into the gas phase during photolysis were detected and their energy distributions measured by TOF-QMS. Thus, we have attempted to more fully characterize reaction products that are ejected into the gas phase *and* those that remain in the film, something that has not been previously done.

1. Reflection Absorption Infrared Spectroscopy (RAIRS). Figure 1a shows the RAIR spectrum recorded for a 70 ML film of CH_3I on Ag(111) at 2 cm^{-1} resolution. The assignment for the CH_3I thin film spectrum can be made by comparison to solid CH_3I[27] (Table 1). Also shown in Table 1 are the absorption band frequencies for a CH_3I thin film adsorbed on Pt(111).[28] There are only minor differences between the band frequencies for CH_3I multilayers on Ag(111) and those for CH_3I on Pt(111) and for crystalline CH_3I. The spectrum recorded for a 70 ML film of CD_3I is shown in Figure 1b. The infrared absorption bands shift as expected for the deuterated molecule. The assignment of the infrared bands for CD_3I is given in Table 1 along with the isotope shift (ν_H/ν_D) for each of the bands.

Figure 2 shows a series of expanded RAIR spectra taken of a 70 ML film of CH_3I before and after irradiation with an increasing number of photons incident on the film. Only the spectral range where new peaks are most evident upon photolysis is shown (950−1550 cm^{-1}). The bottom spectrum labeled **a** is that of the film prior to irradiation. As the number of incident photons increases, several new bands appear in the spectra. Most obvious in the spectra are new absorption bands at frequencies near 1110 and 1299 cm^{-1}. The band at 1110 cm^{-1} is assigned to the CH_2 twisting mode of methylene iodide, CH_2I_2. This assignment is in good agreement with the liquid-phase value of 1099 cm^{-1}.[29] The band at 1299 cm^{-1} is assigned

TABLE 1: Vibrational Assignment of CH_3I Thin Films

mode description	crystalline CH_3I[a]	CH_3I–Pt(111)[b]	CH_3I–Ag(111)[c]	CD_3I–Ag(111)[c]	ν_H/ν_D[d]
$\nu_a(C-H)$	3047, 3034	3047, 3035	3036	2283	1.33
$\nu_s(C-I) + 2\nu_s(CH_3)$	n.o.[e]	n.o.	2946	2137	1.38
$\nu_s(C-H)$	2933	2934	2935	2128	1.38
$2\delta_a(CH_3)$	2834	2833	2834	n.o.	
$2[\nu_s(C-I) + \rho(CH_3)]$	2812, 2803	2803, 2776	2803, 2777	2052	1.37, 1.35
$2\delta_s(CH_3)$	2456	2456	2457	n.o.	
$\delta_s(CH_3) + \rho(CH_3)$	2128, 2120	n.o.	2124	n.o.	
$\delta_a(CH_3)$	1425, 1420	1427	1426	1042	1.37
$\nu_s(C-I) + \rho(CH_3)$	1401, 1396	1403	1401	984	1.42
$2\delta_s(CH_3)$	1240, 1235	1236	1238	942	1.31
$2\nu_s(C-I)$	1040, 1028	1040	1040	n.o.	
$\rho(CH_3)$	895, 887	897, 886	896, 887	n.o.	
$\nu_s(C-I)$	519, 523	n.o.	n.o.	n.o.	

[a] Reference 27. [b] Reference 28. [c] This work. [d] ν_H/ν_D is calculated using the CH_3I–Ag(111) and CD_3I–Ag(111) frequencies. [e] n.o. = not observed.

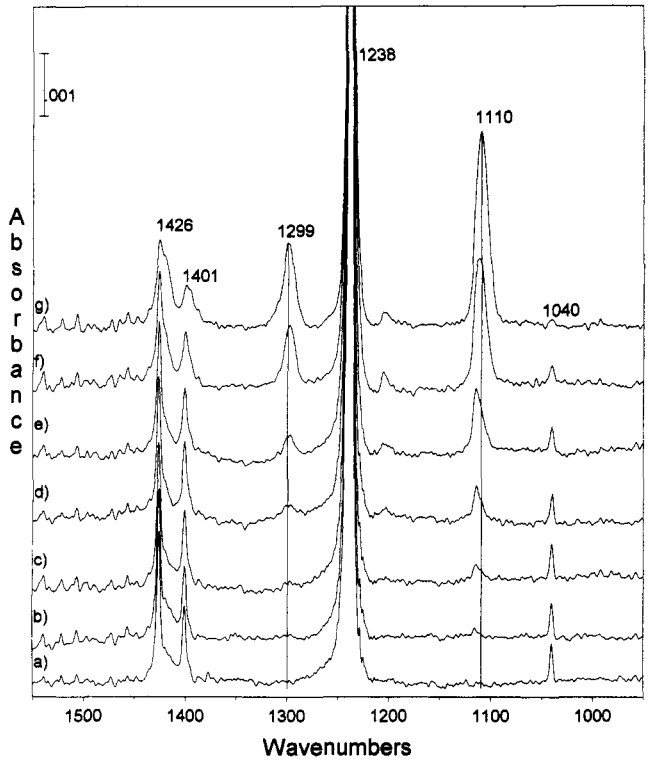

Figure 2. 2 cm^{-1} resolution RAIR spectra for a CH_3I thin film adsorbed on Ag(111) at 100 K as a function of photolysis: (a) 70 ML film, no irradiation and after (b) 1.4×10^{17} (c) 2.6×10^{17}; (d) 5.3×10^{17}; (e) 1.1×10^{18}; (f) 2.6×10^{18}; and (g) 6.6×10^{18} photons/cm^2. The laser fluence was constant at 0.9 mJ/cm^2 in these experiments.

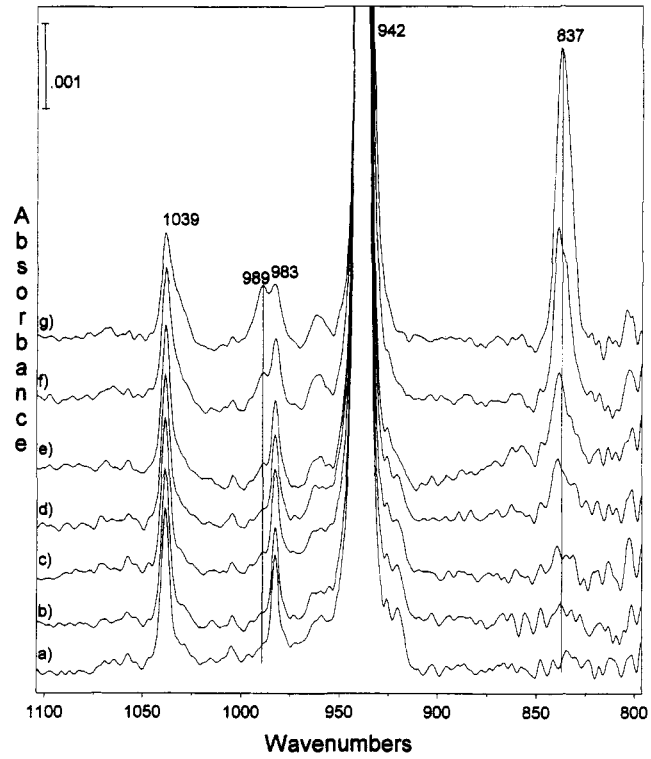

Figure 3. 2 cm^{-1} resolution RAIR spectra for a CD_3I thin film adsorbed on Ag(111) at 100 K as a function of photolysis: (a) 70 ML film, no irradiation and after (b) 1.4×10^{17}; (c) 2.6×10^{17}; (d) 5.3×10^{17}; (e) 1.1×10^{18}; (f) 2.6×10^{18}; and (g) 6.6×10^{18} photons/cm^2. The laser fluence was constant at 0.9 mJ/cm^2 in these experiments.

to the deformation mode of CH_4, in good agreement with the gas-phase value of 1306 cm^{-1}.[30] In addition to the growth of bands at 1110 and 1299 cm^{-1} upon irradiation, some of the parent absorption bands broaden and shift in frequency upon photolysis.

The above band assignments are supported by the corresponding experiment using CD_3I. The expanded CD_3I RAIR spectra as a function of irradiation are shown in Figure 3. Two bands grow in upon irradiation near 837 and 989 cm^{-1} and are assigned to CD_2I_2 and CD_4, respectively. The observed shifts correspond to the predicted shifts for deuterium substitution of these molecules.

The integrated areas of the infrared absorption bands of CH_3I (2935 cm^{-1}), CH_2I_2 (1110 cm^{-1}), and CH_4 (1299 cm^{-1}) as a function of the number of photons incident on the film are shown in Figure 4. Initially, loss of the CH_3I band at 2935 cm^{-1} was concurrent with the growth of the CH_2I_2 band at 1110 cm^{-1} and the CH_4 band at 1299 cm^{-1}. The integrated areas of the CH_2I_2 and CH_4 bands rise to a maximum at approximately 0.8×10^{19} photons/cm^2 and then decrease as irradiation continues. The dependencies of the integrated areas as a function of the number of incident photons for the two photoproducts have different shapes, particularly after irradiation with many photons indicating that they are indeed two separate photoproducts. The CH_4 and CH_3I integrated areas level off and the CH_2I_2 integrated area continues to decrease.

In a separate experiment, multilayers of CH_2I_2 were adsorbed on Ag(111) and then photolyzed. Figure 5a–c shows the RAIR spectra of CH_2I_2 at three different gas exposures, 10, 25, and 100 langmuirs. The most intense feature is a band at 1109 cm^{-1}, a weaker band is evident at 3041 cm^{-1} and another band at 2965 cm^{-1} is observed only for the 100 langmuir exposure film. The 1109 cm^{-1} band is assigned to the CH_2 twisting mode, and the two bands at 3041 and 2965 cm^{-1} are assigned to the C–H asymmetric and symmetric stretching modes, respectively.

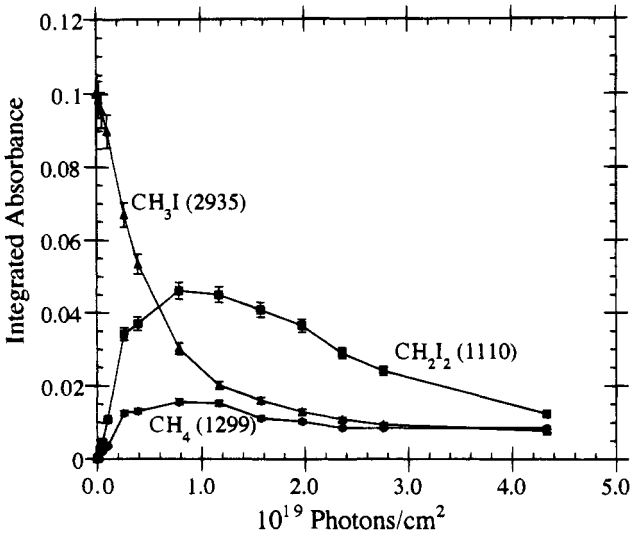

Figure 4. Integrated absorbance of the infrared bands for CH_3I, CH_2I_2, and CH_4 plotted as a function of the number of photons incident on the film.

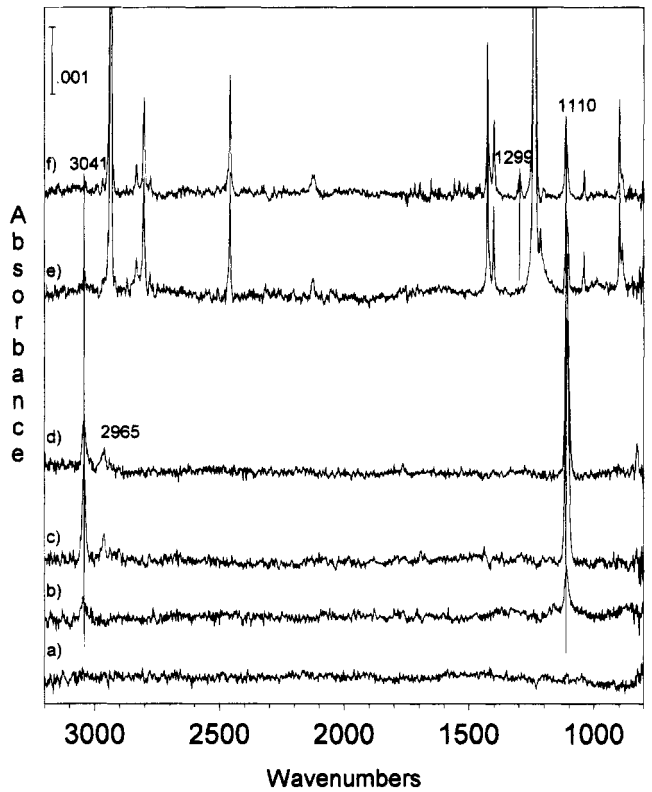

Figure 5. RAIRS spectra of CH_2I_2 thin films: (a) 10 (b) 25, and (c) 100 langmuir exposures; (d) after irradiation of the 100 langmuir exposure film. RAIRS spectra of CH_2I_2 (15 langmuir exposure) codosed with CH_3I (210 langmuir exposure): (e) codosed film before irradiation and (f) codosed film after irradiation at 248 nm.

Although no photolysis products were identified in RAIRS after 248 nm irradiation of 100 langmuir exposure film (Figure 5d), and loss of only CH_2I_2 was seen, some production of CH_4 and CH_3I from the irradiated CH_2I_2 film was observed in TPD. The formation of CH_4 and CH_3I from CH_2I_2 photolysis may explain why the CH_4 and CH_3I infrared signals level off as the CH_3I film is photolyzed for long periods. The data indicate that a steady state may be established for these two species, CH_4 and CH_3I. The lack of establishment of a steady state for CH_2I_2 suggests a higher photodissociation cross section for this molecule compared to that of CH_3I.

The RAIR spectra recorded of a CH_2I_2 film and a codosed film of CH_3I and CH_2I_2 also provide further RAIRS evidence for the identification of the CH_3I film photoproducts. A codosed film of CH_3I (210 langmuirs) with CH_2I_2 (15 langmuirs) is shown in Figure 5e. After 248 nm irradiation of the codosed film there is a small increase in intensity of the 1110 cm^{-1} band and the appearance of a new band at 1299 cm^{-1} assigned to CH_4 (Figure 5f). The RAIRS data for a CH_2I_2 film and CH_2I_2/CH_3I film before and after irradiation provide definitive evidence that the two absorption bands at 1110 and 1299 cm^{-1} are due to two different photoproducts and that CH_2I_2 is one of those products. TPD data as discussed below corroborate the RAIRS data.

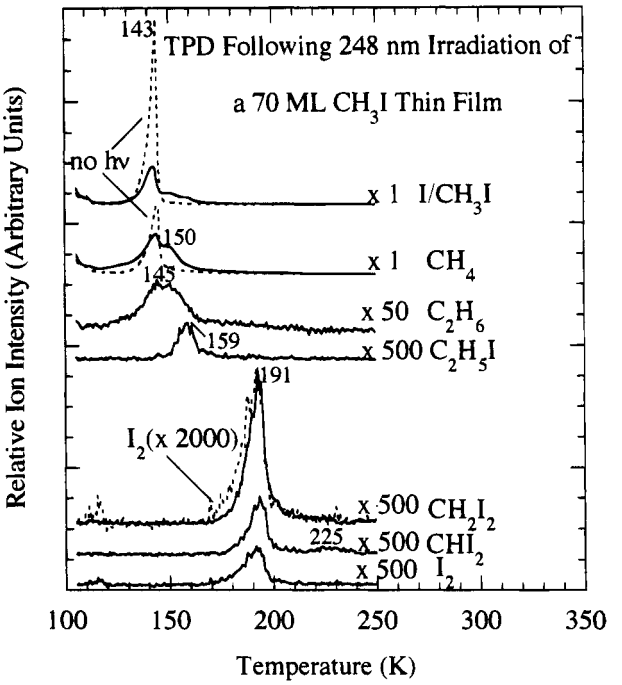

Figure 6. TPD spectra of a 70 ML CH_3I film after irradiation with approximately 7×10^{18} photons/cm^2. The parent ion was monitored for each of the molecular species shown above except for CH_3I. An ion fragment of CH_3I (*m/e* = 127) was monitored so as to use the same QMS amplifier range as that of CH_4. Before and after irradiation with 7×10^{18} photons/cm^2, the *m/e* = 127 ion signal tracked the *m/e* = 142 ion signal.

2. Temperature Programmed Desorption (TPD). Post-irradiation TPD was used to confirm the photoproducts detected by RAIRS. Figure 6 shows the TPD spectra after irradiation of 70 ML CH_3I with approximately 7×10^{18} photons/cm^2. The TPD spectra show desorption peaks for CH_4 and CH_2I_2, the two products detected in RAIRS. Note that although some CH_4 signal is observed without photolysis, its intensity exactly tracks that of CH_3I (and CH_3I ion fragments), i.e., it appears to form in the ionizer of the mass spectrometer. After photolysis, however, CH_4 desorption does not track CH_3I (and CH_3I ion fragments) at all temperatures, indicating that CH_4 itself is desorbing from the film thus confirming it as a photoproduct. Some C_2 products are detected in TPD as well. C_2H_6 and C_2H_5I desorb with desorption rate maxima near 145 and 159 K. Both of these desorption peaks are not present if the sample is not irradiated, confirming that they are indeed photoproducts.

There is some evidence for the desorption of CHI_3 and I_2 from the surface after irradiation. The parent ion for CHI_3 is outside the range of our mass spectrometer; however, a small but reproducible peak at 225 K is seen in the CHI_2^+ desorption trace. CHI_2^+ is an expected fragment of CHI_3, and the weak peak at 225 K suggests some formation of iodoform in the film. Although the parent ion for molecular iodine, I_2^+, has a desorption rate maximum at the same temperature as that of

$CH_2I_2^+$, the I_2^+ signal does not exactly track the $CH_2I_2^+$ signal. There is some additional I_2 desorption at lower temperatures that is not associated with fragmentation of CH_2I_2, suggesting that I_2 is formed and retained in the film as well. No desorption features corresponding to molecular CH_2I_2, I_2, and CHI_3 are present without irradiation, indicating that these molecular species are also photoproducts.

Not shown, but observed, is the desorption of atomic iodine ($m/e = 127$) at approximately 620 K, a value in good agreement with that given for the desorption of I from photolysis of at least two monolayers of CH_3I on Ag(111).[21] The desorption of C_2H_6 at approximately 270 K from CH_3 coupling reactions on Ag(111) is also observed, but not shown.[25]

3. Time-of-Flight Quadrupole Mass Spectrometry (TOF-QMS). For the following experiments, a 70 ML film of CH_3I was irradiated with 248 nm at a laser fluence of 0.9 mJ/cm^2. Under these conditions, three species desorbed from the surface during irradiation: CH_3, atomic I, and CH_3I. Figure 7 shows the TOF distributions of these three photoproducts. Each spectrum represents the first 1200 laser pulses at 0.9 mJ/cm^2 per pulse on a freshly dosed CH_3I film. The CH_3I spectrum was obtained at a gain seven times higher than the gain for the CH_3 and I spectra. Some of the TOF distributions were fit by Maxwell–Boltzmann distributions using the method described by Wedler and Ruhman.[31]

Figure 7a shows the early time portion of the CH_3 TOF distribution. Two CH_3 photofragment peaks corresponding to production of iodine atoms in the $I(^2P_{3/2})$ and $I^*(^2P_{1/2})$ states are observed at 47 and 59 μs, respectively. These two peaks are very narrow, whereas the tail of the CH_3 distribution is broader and can be fit by a distribution with a temperature of 3200 K. These slower methyl fragments may be due to methyl fragments that have undergone one or more collisions before escaping from the film surface. A much broader, late peak in the distribution (not shown) was also observed due to the fragmentation of photodesorbed CH_3I in the ionizer of the mass spectrometer. The TOF distribution of photodesorbed CH_3I (Figure 7c) peaks at approximately 450 μs and is adequately fit by a single Maxwell–Boltzmann distribution with a temperature of 1170 K. The atomic I distribution (Figure 7b) peaks at an earlier time (396 μs) than does the CH_3I distribution, indicating that the observed I signal is not just a result of fragmentation of CH_3I in the ionizer of the mass spectrometer. In a separate experiment, we determined that the contribution to the I atom signal from CH_3I fragmentation is less than 10%. Therefore, the I distribution could be satisfactorily fit by a single Maxwell–Boltzmann distribution for mass 127 with a temperature of 1400 K.

The dependence of the primary photoproduct TOF signals on laser fluence is shown in Figure 8. These data were obtained in experiments without the beam-expanding lens, but with lower laser fluence so that the maximum fluence was 1.0 mJ/cm^2. The slope of the line, n, was calculated from each of the plots. The photoyields of CH_3 and I exhibit a nearly linear dependence on laser fluence, indicating that the photodissociation of CH_3I in multilayers is a one-photon process, as seen in the gas phase. The CH_3I yield exhibited a linear dependence on laser fluence as well, and the CH_3I signal could still be detected at one-tenth of the maximum laser fluence.

Additional gas-phase species besides CH_3I, CH_3, and I were detected when the pulse energy of the laser was increased to 3.2 mJ/cm^2 by removing the beam expanding lens. CH_4 desorption was observed promptly upon irradiation, but its signal decayed away very quickly. The desorption of I_2 and CH_2I_2 grew in as photolysis progressed and then slowly decayed away.

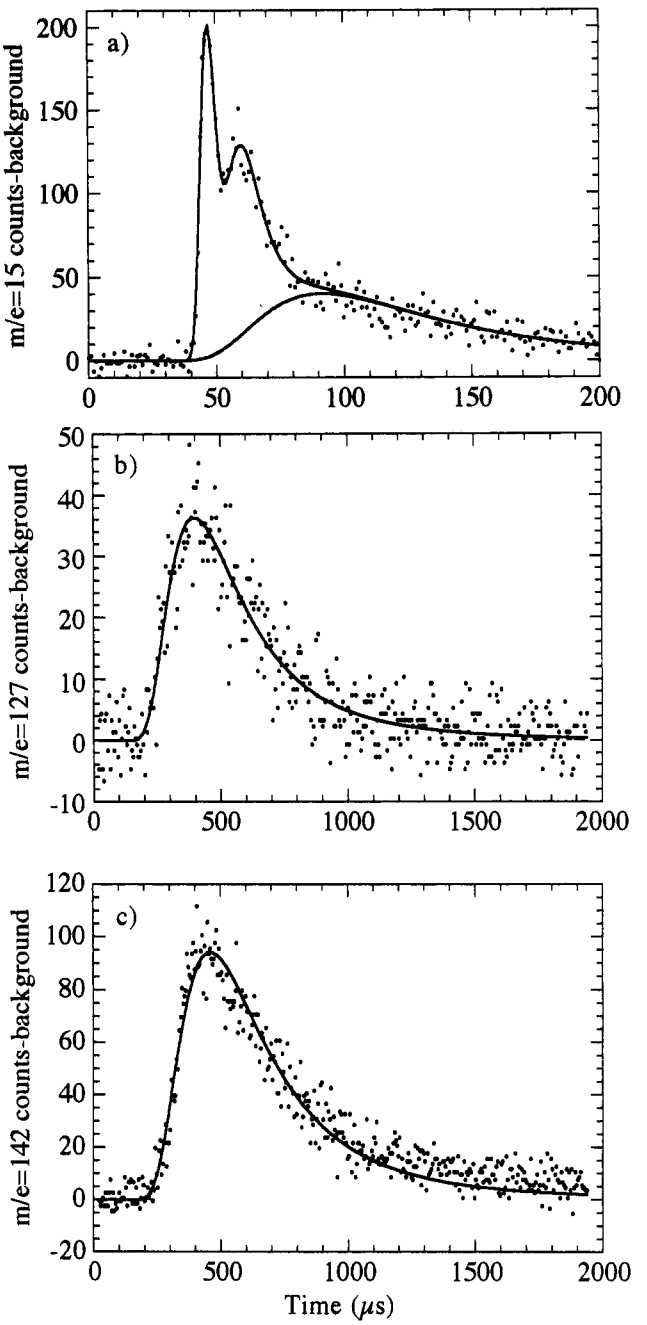

Figure 7. TOF-QMS spectra of (a) CH_3, (b) I, and (c) CH_3I photoejected from a 70 ML CH_3I film. Each spectrum was acquired by summing the signal from 1200 laser pulses at a laser fluence of 0.9 mJ/cm^2.

No evidence of CH_3CH_2I, C_2H_6, or HI desorption was found. TOF distributions measured for each of the desorbing species, CH_4, I_2, and CH_2I_2, are shown in Figure 9. These are the first reported distributions of any of these species from photolysis of CH_3I multilayers adsorbed on a metal surface. The CH_4 distribution (Figure 9a) peaks at approximately 390 μs and is adequately fit by a Maxwell–Boltzmann distribution corresponding to a temperature of 184 K. The CH_4 signal cannot be solely a result of the fragmentation or reaction of any of the other photoproducts. If it were, it would have the same velocity distribution as the parent photoproduct. The only other photoproduct which has a similar velocity distribution is the atomic I. The I_2 and CH_2I_2 distributions (Figure 9b,c) peak at approximately 1000 μs. Both TOF distributions can be fit by a Maxwell–Boltzmann distribution corresponding to temperatures of 365 K for I_2 and 331 K for CH_2I_2. I_2 has been

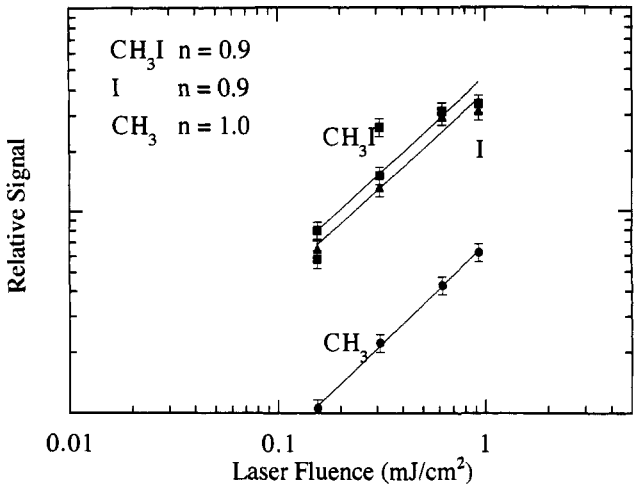

Figure 8. Log−log plot of the ion signal versus the laser fluence. The data can be fit with a straight line of slope, n, approximately equal to one.

observed from the photodissociation of gas-phase CH_3I clusters at 248 nm and other wavelengths,[5−9] and an I_2^+ nonresonant photoionization signal was seen in the 257 nm photodissociation of CH_3I multilayers on MgO.[13] By turning off the electron emission in the ionizer of the mass spectrometer, we can test for the direct photoproduction of ions. We see no evidence of I_2^+ desorbing directly from the surface. The laser fluence dependence of the CH_4, I_2, and CH_2I_2 signals is strongly nonlinear. None of these species were detected in the gas phase using the beam-expanding lens.

The dependence of the TOF signal for all of the gas-phase photoproducts on the number of photons incident on the film is shown in Figure 10. Scaling of the data for the different species relative to one another is arbitrary. For the photoproducts CH_3, I, and CH_3I, the data were taken with the expanded laser beam (0.9 mJ/cm^2). The total CH_3 signal from photodissociation of CH_3I increases initially and then decreases approximately exponentially with photon fluence. The I signal shows the same type of photon fluence dependence as does CH_3 in that it increases slightly at first and then decreases approximately exponentially. However, the I signal begins its decrease at a smaller total fluence and has a steeper fluence dependence than does the CH_3 signal. The yield of CH_3I stays nearly constant initially, then decreases approximately exponentially, although there is an indication that the rate of gas phase CH_3I production is changing with photon fluence. For the photoproducts CH_4, I_2, and CH_2I_2, the data were obtained without the beam-expanding lens. The I_2 and CH_2I_2 signals behave similarly in that the TOF signals for both species initially increase to a maximum, then decrease as photolysis proceeds. The CH_4 signal has the most interesting behavior of any photoproduct. The signal is highest initially, even though the infrared data shows that CH_4 grows in approximately as the CH_2I_2 does.

Discussion

1. Review of Thermal Chemistry and Photochemistry for 1 and 2 ML of CH_3I on Ag(111). The thermal chemistry and photochemistry of CH_3I on Ag(111) at low coverages, 1 to 2 ML, has been carefully investigated by White and co-workers.[21,25] At 100 K, CH_3I adsorbs molecularly with the iodine end of the molecule bonded to the Ag surface. Upon warming, CH_3I dissociates to give methyl groups that recombine near 260 K to form ethane which desorbs into the gas phase. Iodine desorbs at much higher temperatures near 800 K.[25] The

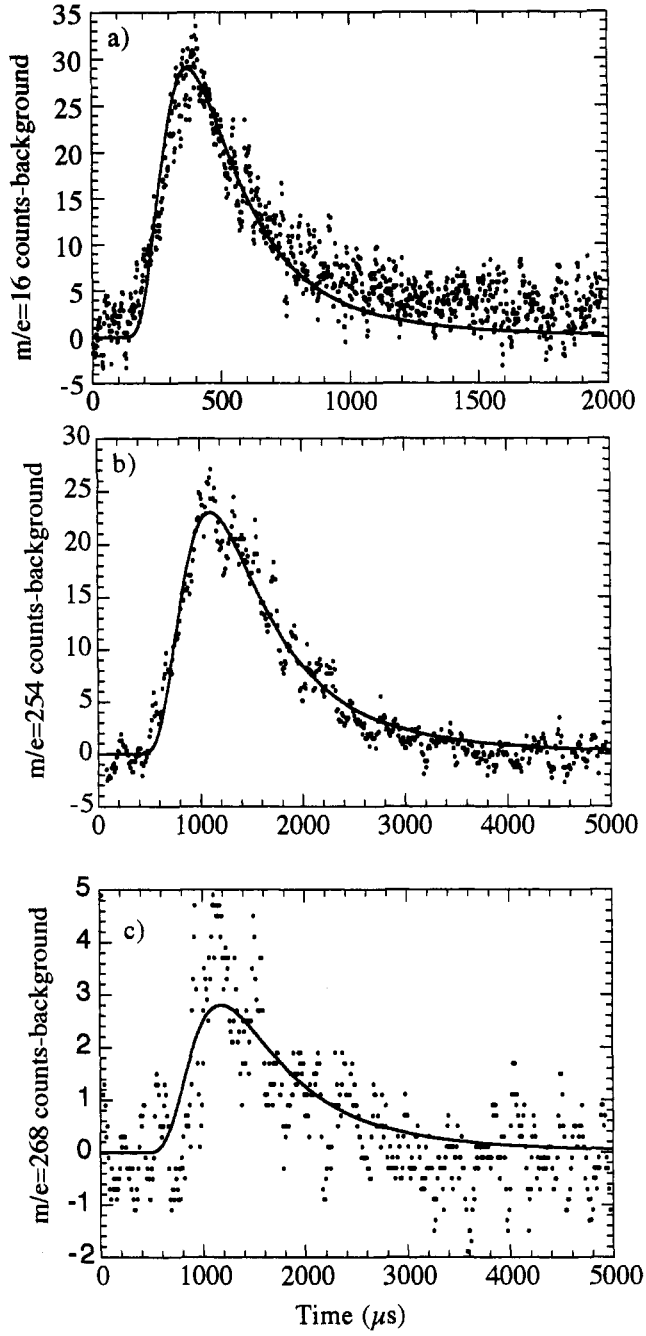

Figure 9. TOF-QMS spectra for (a) CH_4, (b) I_2, and (c) CH_2I_2 photoejected from a 70 ML CH_3I film. Each spectrum was acquired by summing the signal from 1200 laser pulses at 3.2 mJ/cm^2.

mechanism of the surface photochemistry of CH_3I on Ag(111) has been determined by Zhou and White to be predominantly substrate mediated in the low-coverage regime.[25] Jensen and Polanyi investigated the TOF distribution of the methyl fragments and also conclude that a substrate-mediated mechanism could account for the photochemistry of adsorbed methyl iodide below five monolayers.[15] Upon photolysis with a broadband Hg arc lamp CH_3I dissociates to give CH_3 and I. Zhou and White have shown that most of the CH_3 fragments desorb into the gas phase whereas I and CH_3I do not, presumably because of the orientation of the CH_3I molecules. The iodine atom is bonded to the surface in adsorbed methyl iodide, and iodine does not desorb into the gas phase but remains on the surface. A preferred orientation of CH_3I with the iodine end of the molecule directed toward the surface appears to be operative in the second layer as well.[21]

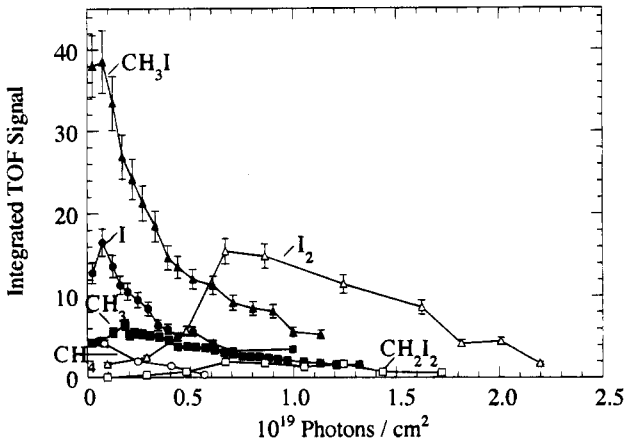

Figure 10. Flux-weighted integrated TOF signal for the gas-phase photoproducts CH_3I, I, CH_3, CH_4, CH_2I_2, and I_2 plotted as a function of the number of photons incident on the film. The laser fluence was 0.9 mJ/cm^2 for CH_3I, I, and CH_3 TOF data and 3.2 mJ/cm^2 for CH_4, CH_2I_2, and I_2. The data collected for gas-phase photoproducts at a laser fluence of 0.9 mJ/cm^2 are represented by filled symbols: CH_3I, ▲; I, ●; CH_3, ■. The data collected for gas-phase photoproducts at a laser fluence of 3.2 mJ/cm^2 are represented by open symbols: I_2, △; CH_4, ○; CH_2I_2, □.

SCHEME 1. Photoproducts from 248 nm Irradiation of CH_3I Thin Films

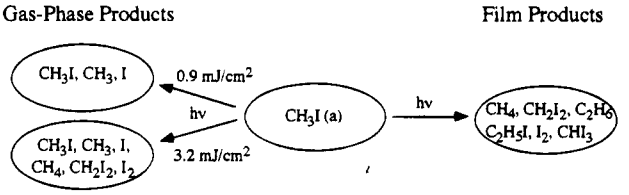

2. CH_3I Thin Film Photochemistry on Ag(111) at 248 nm: Photoproduct Identification and Reaction Mechanisms. In the high-coverage multilayer or thin film regime, interactions between neighboring methyl iodide molecules play a role in the photochemistry, whereas substrate effects become less important. Previous work has shown that the photodynamics of multilayers of CH_3I can be understood in terms of a direct excitation of the adsorbed molecule,[15,17-19] and CH_3I molecules in the film at the film/vacuum interface have an antiparallel orientation.[17-19] As we have shown in the Results section, direct excitation of the CH_3I molecules in the film can also initiate subsequent reactions. A discussion of the photochemistry and dynamics in the CH_3I film to produce retained products and at the CH_3I film surface to give gas phase products is given below.

Reaction products detected by RAIRS, TPD, and TOF-QMS are summarized in Scheme 1. Both gas-phase products and products that are retained in the film are shown. Two major photoproducts retained in the methyl iodide film after 248 nm irradiation have been identified by RAIRS and TPD as CH_2I_2 and CH_4. Additional photoproducts retained in film have been identified by TPD, including C_2H_6, CH_3CH_2I, CHI_3, and I_2. In the film, the initial reaction is similar to the gas-phase photodissociation of CH_3I to form two radical species, methyl radicals and iodine atoms (eq 1). Photolysis reactions to form CH_2 and HI have been previously determined to be of minor importance at 248 nm.[32]

$$CH_3I \xrightarrow{h\nu} CH_3 + I \quad (1)$$

Subsequent radical reactions in the film lead to the formation of additional photoproducts. Reactions 2–8 involve radical reactions that are proposed to be involved in the formation of the observed photoproducts.

$$CH_3 + CH_3I \rightarrow CH_4 + CH_2I \quad (2)$$

$$CH_2I + I \rightarrow CH_2I_2 \quad (3)$$

$$CH_3 + CH_3 \rightarrow C_2H_6 \quad (4)$$

$$CH_2I + CH_3 \rightarrow C_2H_5I \quad (5)$$

$$I + I \rightarrow I_2 \quad (6)$$

$$CHI_2 + I \rightarrow CHI_3 \quad (8)$$

$$CH_3 + CH_2I_2 \rightarrow CH_4 + CHI_2 \quad (7)$$

In the reaction shown in eq 2, CH_4 is produced from abstraction of hydrogen from CH_3I by hot methyl radicals. Given the low enthalpy of vaporization of methane (8.2 kJ/mol), it may seem surprising that CH_4 should remain in the film at all. However, it should be noted that methane is not being retained in a methane film, but rather it is a methyl iodide film. The intermolecular forces between the polar methyl iodide and nonpolar methane are greater than those for the methane–methane interaction, and the data indicate that the CH_3I–CH_4 interaction is large enough for methane to be retained in the film. In fact, the data show that as the film is irradiated for an extended period of time, methane is removed from the film. The integrated areas of the CH_3I and CH_4 bands track each other very closely after a photon fluence of 1.2×10^{19} photons/cm^2 is reached (Figure 4), suggesting that the CH_4 loss is correlated at higher photon fluences with loss of the CH_3I film.

Gas-phase products are detected from the photochemistry taking place at the film/vacuum interface. At low laser fluence near 0.9 mJ/cm^2 per pulse, only CH_3I, CH_3, and I desorb from the surface. The dependence of the product ion signal in TOF-QMS on laser fluence shows that these species, CH_3I, CH_3, and I, desorb following the absorption of a single photon.

Although the details of our TOF-QMS data will be published at a later date,[33] it is apparent that the gas-phase photoproducts desorb with appreciable energy. Two peaks in the methyl spectrum correlate with the production of $I(^2P_{3/2})$ and $I^*(^2P_{1/2})$ having mean translational energies of approximately 1.9 and 1.2 eV, respectively. The tail at longer times can be fit to a Maxwell–Boltzmann distribution of a temperature near 3200 K and is tentatively attributed to methyl fragments that have undergone one or more collisions before escaping from the film surface. Although there is no reason a priori to fit the data to a Maxwell–Boltzman distribution, we have fit some of the curves to this functional form. The TOF distribution of photodesorbed CH_3I and I can also be adequately fit by a single Maxwell–Boltzmann distribution with temperatures of 1170 and 1400 K, respectively.

At higher laser fluences, additional products are detected desorbing from the film. CH_4, I_2, and CH_2I_2 are produced in the gas phase at laser fluences near 3.2 mJ/cm^2. These three species, CH_4, I_2, and CH_2I_2, desorb with much less energy. The CH_4 distribution is adequately fit by a Maxwell–Boltzmann distribution corresponding to a temperature of 184 K. The I_2 and CH_2I_2 distributions can be fit by single Maxwell–Boltzmann distributions corresponding to temperatures of only 365 K for I_2 and 331 K for CH_2I_2.

The origins of gas-phase CH_4, I_2, and CH_2I_2 signals are not well understood. An I_2^+ photoionization signal was seen by Trentelman et al.[13] from 257 nm irradiation of CH_3I adsorbed

on MgO(100). This signal was not a time-of-flight signal; rather they monitored the background I_2^+ signal as photolysis progressed. Their results show the same behavior as is seen for I_2 in our photon fluence dependence (Figure 10). They determined that the desorbing species could not be ground state molecular iodine because it showed none of the optical absorption features of that molecule. Trentelman et al. postulated that I_2^+ was formed by the photodissociation of a larger molecule or molecules. It is tempting to say that CH_2I_2 is that larger molecule, since I_2 and CH_2I_2 have similar TOF distributions. We also know that I_2 is a fragment of CH_2I_2 in the quadrupole mass spectrometer, so it seems reasonable to hypothesize that the CH_2I_2 photoproduct is being ejected into the gas phase and then fragmenting to I_2^+ in the mass spectrometer. However, experiments done to test this hypothesis have determined that this is not the case. The mass spectrum of CH_2I_2 was measured, and it was found that the (m/e = 254):(m/e = 268) ratio was less than 1. However, it is clear from Figure 9 that the m/e = 254 TOF signal is much larger than that for m/e = 268. Another experiment gave further evidence that the (m/e = 254) signal cannot come solely from photodesorption and fragmentation of CH_2I_2. Thin films of CH_2I_2 were adsorbed on Ag(111), and TOF distributions were measured. No evidence for ejection of CH_2I_2 or I_2 into the gas phase was found even at high laser fluences. Instead, very large TOF signals for I and CH_2I were observed, along with a very small CH_2 signal. It appears that CH_2I_2 photodissociates but does not photodesorb. It is therefore proposed that both I_2 and CH_2I_2 are photofragments or cracking fragments of some larger molecule or molecules. One possibility for the identity of this species is some derivative of a CH_3I cluster. It is unlikely that CH_3I clusters themselves are the precursors for the I_2^+ and $CH_2I_2^+$ signals, because if so, these signals should be detected immediately upon beginning photolysis, instead of growing in as they do. A species such as $CH_3I_2^+$ could be the precursor to the observed I_2^+ and $CH_2I_2^+$ TOF signals. Feldmann et al.[34] noted that using single-photon ionization of the desorbed flux in the "explosive" desorption regime (> 1.5 mJ/cm^2 at 266 nm), they observed a dominant contribution to the flux of CH_3I and "cluster ions like $CH_3I_2^+$". Trentelman et al. proposed a product cluster that was rich in iodine as well.[13] It seems likely that the formation of these clusters is facilitated by the buildup of some photoproduct in the film, possibly atomic iodine. Therefore, the maximum TOF signal for the fragments of these clusters would come at some intermediate photolysis time, as observed. It is clear that the CH_4 signal has yet another, albeit unknown, origin.

3. Photolysis Cross Section of CH_3I at 248 nm. The total photolysis cross-section for loss of CH_3I from photochemistry occurring in the film and at the film surface can be determined from the infrared data (Figure 4). Only the first eight data points of Figure 4 are used to construct the plot shown in Figure 11, i.e., from (0.0 to 0.8) × 10^{19} photons/cm^2, before secondary photoreactions become important. There is approximately 70% loss of CH_3I molecules after irradiation with 0.8 × 10^{19} photons/cm^2. Assuming the integrated absorbance is proportional to the number of adsorbed molecules, then

$$\sigma = -\frac{\ln(N/N_0)}{\text{number of photons/cm}^2} \qquad (9)$$

where σ is the photolysis cross section, N is the number of molecules remaining in the film, and N_0 is the number of molecules initially in the film.

A plot of $\ln(N/N_0)$ versus the number of photons per square centimeter incident on the film is shown in Figure 11. The photolysis cross section for CH_3I at 248 nm is determined to be (1.6 ± 0.1) × 10^{-19} cm^2 from this analysis. This value is approximately 10 times smaller than the cross section calculated from the absorption cross section for gas-phase CH_3I.[35] The smaller cross section is somewhat expected considering that there is likely some quenching near the vicinity of the metal surface. Zhou and White calculated a cross section of (2.8 ± 0.6) × 10^{-20} cm^2 from broadband irradiation of 1 ML of CH_3I on Ag(111).[21] Cage effects in the film itself will also cause a lower cross section for loss of CH_3I as well.[36,17]

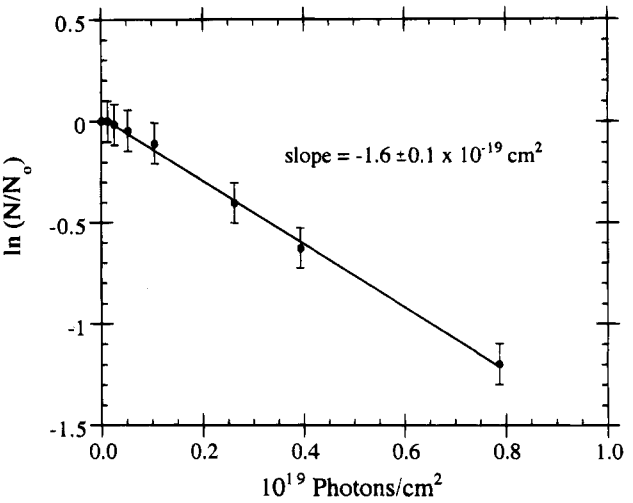

Figure 11. $\ln(N/N_0)$ plotted as a function of the number of photons incident on the film. The cross section is calculated from the slope of the line to be (1.6 ± 0.1) × 10^{-19} cm^2.

4. I and I* Branching from CH_3I Photodissociation. In the TOF spectra of CH_3, we see evidence that the gas-phase dynamics are still active at the film surface although they are altered. The branching into the two different channels (I and I*) can be determined from integrated areas of the peaks when flux is plotted vs energy. $\Phi^* = I^*/(I + I^*)$ is initially calculated to be 0.52 ± 0.05, below the gas-phase value of 0.73.[36,37] Similar changes in Φ^* have been observed for CH_3I films on metal and oxide surfaces.[11,15,19] The Φ^* is dependent on film thickness and does change upon irradiation.[17,33]

Conclusions

Using RAIRS, TPD, and TOF-QMS, we have established that 248 nm photolysis of a multilayer film of CH_3I on Ag(111) produces products that are retained in the film, including CH_2I_2, CH_4, C_2H_6, CH_3CH_2I, CHI_3, and I_2, as well as products that desorb from the film. CH_3, I, and CH_3I desorb from the film into the gas phase at all laser fluences. In the TOF spectra of the gas-phase product CH_3, we see evidence that the gas-phase dynamics are still active but altered at the film surface. At high laser fluences, the presence of clusters in the desorbing flux may be responsible for the I_2 and CH_2I_2 TOF signals observed.

Acknowledgment. The authors acknowledge the support of the National Science Foundation (9309731). K.B.M. thanks the General Electric Foundation for support in the form of a General Electric Graduate Fellowship.

References and Notes

(1) Harris, G. M.; Willard, J. E. *J. Am. Chem. Soc.* **1954**, *76*, 4678.
(2) Souffie, R. D.; Williams, R. R., Jr.; Hamill, W. H. *J. Am. Chem. Soc.* **1956**, *78*, 917.
(3) Barker, P. G.; Purnell, J. H.; Young, B. C. *Trans. Faraday Soc.* **1970**, *66*, 2244.
(4) Donaldson, D. J.; Vaida, V. *J. Chem. Phys.* **1987**, *87*, 2522.
(5) Sapers, S. P.; Vaida, V. *J. Chem. Phys.* **1988**, *88*, 3638.
(6) Syage, J. A.; Steadman, J. *Chem. Phys. Lett.* **1990**, *166*, 159.

(7) Wang, P. G.; Zhang, Y. P.; Ruggles, C. J.; Ziegler, L. D. *J. Chem. Phys.* **1990**, *92*, 2806.

(8) Fan, Y. B.; Donaldson, D. J. *J. Chem. Phys.* **1992**, *97*, 189.

(9) Fan, Y. B.; Randall, K. L.; Donaldson, D. J. *J. Chem. Phys.* **1993**, *98*, 4700.

(10) Vaidyanathan, G.; Lyktey, M. Y. M.; Stry, J. J.; DeLeon, R. L.; Garvey, J. F. *J. Phys. Chem.* **1994**, *98*, 7475.

(11) Kutzner, J.; Lindeke, G.; Welge, K. H.; Feldmann, D. *J. Chem. Phys.* **1989**, *90*, 548.

(12) Trentelman, K. A.; Fairbrother, D. H.; Stair, P. C.; Strupp, P. G.; Weitz, E. *J. Vac. Sci. Technol. A* **1991**, *9*, 1820.

(13) Trentelman, K. A.; Fairbrother, D. H.; Strupp, P. G.; Stair, P. C.; Weitz, E. *J. Chem. Phys.* **1992**, *96*, 9221.

(14) McCarthy, M. I.; Gruber, R. B.; Trentelman, K. A.; Strupp, P.; Fairbrother, D. H.; Stair, P. C.; Weitz, E. *J. Chem. Phys.* **1992**, *97*, 5168.

(15) Jensen, E. T.; Polanyi, J. C. *J. Phys. Chem.* **1993**, *97*, 2257.

(16) Garrett, S. J.; Holbert, V. P.; Stair, P. C.; Weitz, E. *J. Chem. Phys.* **1994**, *100*, 4615.

(17) Fairbrother, D. H.; Briggman, K. A.; Stair, P. C.; Weitz, E. *J. Phys.Chem.* **1994**, *98*, 13042.

(18) Fairbrother, D. H.; Briggman, K. A.; Weitz, E.; Stair, P. C. *J. Chem. Phys.* **1994**, *101*, 3787.

(19) Fairbrother, D. H.; Briggman, K. A.; Stair, P. C.; Weitz, E. *J. Chem. Phys.* **1995**, *102*, 7267.

(20) Coon, S. R.; Myli, K. B.; Grassian, V. H. *SPIE Proc. SPIE-Int. Soc. Opt. Eng.*, in press. In these proceedings, the laser and photon fluences were erroneously reported to be too large by a factor of 1.33. The correct values are reported here. Also, the flight time through the QMS was incorrectly reported as 18.5 μs instead of the correct value of 20.1 μs reported here.

(21) Zhou, X.-L.; White, J. M. *Surf. Sci.* **1991**, *241*, 270.

(22) Zhou, X.-L., Zhu, X. Y.; White, J. M. *Surf. Sci. Rep.* **1991**, *13*, 73 and references therein.

(23) Ho, W. In *Desorption Induced by Electronic Transitions, DIET IV*; Betz, G., and Varga, P., Eds.; Springer-Verlag: Berlin, 1990; p 48.

(24) Polanyi, J. C.; Rieley, H. In *Dynamics of Gas-Surface Interactions*; Rettner, C. T., Ashfold, M. N. R., Eds.; Royal Society of Chemistry: London, 1991; p 329.

(25) Zhou, X.-L.; Solymosi, F.; Blass, P. M.; Cannon, K. C.; White, J. M. *Surf. Sci.* **1989**, *219*, 294.

(26) Harris, T. D.; Lee, D. H.; Blumberg, M. Q.; Arumainayagam, C. R. *J. Phys.Chem.* **1995**, *99*, 9530.

(27) Kopelman, R. *J. Chem. Phys.* **1966**, *44*, 3547.

(28) Fan, J.; Trenary, M. *Langmuir* **1994**, *10*, 3649.

(29) *The Aldrich Library of FT-IR Spectra*; Pouchert, C. J., Ed.; Aldrich Chemical Co.: Milwaukee, WI, 1985.

(30) Shimanouchi, T. *Tables of Molecular Vibrational Frequencies Consolidated Volume I*; National Bureau of Standards: Washington, DC, 1972.

(31) Wedler, G.; Ruhman, H. *Surf. Sci.* **1982**, *121*, 2464.

(32) Majer, J. R.; Simons, J. P. *Adv. Photochem.* **1964**, *2*, 137.

(33) Coon, S. R.; Myli, K. B.; Grassian, V. H. *To be submitted for publication.*

(34) Feldmann, D.; Kutzner, J.; Welge, K. H. In *Desorption Induced by Electronic Transitions, DIET IV*; Betz, G., Varga, P., Eds.; Springer-Verlag: Berlin, 1990; Vol. 19, p 93.

(35) Calvert, J. G.; Pitts, J. N. *Photochemistry*; Wiley: New York, 1966.

(36) Brus, L. E.; Bondybey, V. E. *J. Chem. Phys.* **1976**, *65*, 71.

(37) Godwin, F. G.; Gorry, P. A.; Hughes, P. M.; Raybone, D.; Watkinson, T. M.; Whitehead, J. C. *Chem. Phys. Lett.* **1987**, *135*, 163.

(38) Godwin, F. G.; Paterson, C.; Gorry, P. A. *Mol. Phys.* **1987**, *61*, 827.

JP951847Y